UCRL -8263

UNIVERSITY OF CALIFORNIA

Radiation Laboratory

TWO-WEEK LOAN COPY

This is a Library Circulating Copy which may be borrowed for two weeks. For a personal retention copy, call Tech. Info. Division, Ext. 5545

BERKELEY, CALIFORNIA

DISCLAIMER

This document was prepared as an account of work sponsored by the United States Government. While this document is believed to contain correct information, neither the United States Government nor any agency thereof, nor the Regents of the University of California, nor any of their employees, makes any warranty, express or implied, or assumes any legal responsibility for the accuracy, completeness, or usefulness of any information, apparatus, product, or process disclosed, or represents that its use would not infringe privately owned rights. Reference herein to any specific commercial product, process, or service by its trade name, trademark, manufacturer, or otherwise, does not necessarily constitute or imply its endorsement, recommendation, or favoring by the United States Government or any agency thereof, or the Regents of the University of California. The views and opinions of authors expressed herein do not necessarily state or reflect those of the United States Government or any agency thereof or the Regents of the University of California.

UCRL-8263

UNIVERSITY OF CALIFORNIA
Radiation Laboratory
Berkeley, California

Contract No. W-7405-eng-48

HELICITY OF THE ELECTRON AND POSITRON IN MUON DECAY

Pierre C. Macq, Kenneth M. Crowe, and Roy P. Haddock

July 29, 1958

Printed for the U.S. Atomic Energy Commission

This report was prepared as an account of Government sponsored work. Neither the United States, nor the Commission, nor any person acting on behalf of the Commission:

A. Makes any warranty or representation, express or implied, with respect to the accuracy, completeness, or usefulness of the information contained in this report, or that the use of any information, apparatus, method, or process disclosed in this report may not infringe privately owned rights; or

B. Assumes any liabilities with respect to the use of, or for damages resulting from the use of any information, apparatus, method, or process disclosed in this report.

As used in the above, "person acting on behalf of the Commission" includes any employee or contractor of the Commission to the extent that such employee or contractor prepares, handles or distributes, or provides access to, any information pursuant to his employment or contract with the Commission.

HELICITY OF THE ELECTRON AND POSITRON IN MUON DECAY

Pierre C. Macq, Kenneth M. Crowe, and Roy P. Haddock

Radiation Laboratory
University of California
Berkeley, California

July 29, 1958

ABSTRACT

The helicity of the electron and positron from muon decay has been measured by determining the sense of circular polarization of their bremsstrahlung by the method of absorption in iron magnetized against or along the direction of motion of the particles. The positron is found to be right-handed and the electron left-handed.

The results are consistent with the two-component neutrino theory, which assumes V, A interaction, conservation of leptons, and left-handed neutrinos.

HELICITY OF THE ELECTRON AND POSITRON IN MUON DECAY*

Pierre C. Macq,† Kenneth M. Crowe, and Roy P. Haddock

Radiation Laboratory
University of California
Berkeley, California

July 29, 1958

I. INTRODUCTION

Since Lee and Yang advanced the hypothesis of the violation of the parity-conservation law in physical phenomena proceeding from weakly interacting particle fields,[1] vigorous theoretical and experimental efforts have been made to clarify understanding of weak interactions. This hypothesis of parity nonconservation doubled the already large number of independent parameters required to describe weak interactions. Landau, Lee, Yang, and Salam have reinvestigated the old and appealing two-component neutrino theory and have shown on the basis of this theory that the number of parameters is halved once we are able to determine the helicity of the neutrino.[2] In the following discussion we assume that the two-component theory applies.

The experiments on the electron distribution from oriented beta sources, on polarization measurements, and on the absence of interference effects in the spectrum shape[3] lead to two possibilities for β decay:

(a) it is of the V and A form of interaction, and emits left-handed neutrinos (the neutrino is defined as the neutral particle emitted in the bound-proton decay), or

(b) it is of the S, T, and P form of interaction, and emits right-handed neutrinos.

A clear choice between these two classes for β decay has been made by Goldhaber et al.[4] They have measured the polarization of the neutrino in electron K capture by the method of resonance scattering of the γ ray. The neutrino is left-handed; therefore, the beta interaction is of the V and A form.

The study of μ decay throws additional light on the weak-interaction phenomena. For we may now ask: Is the hypothesis of lepton conservation consistent with the experimental data of muon decay if we accept a universal

---

*Work done under the auspices of the United States Atomic Energy Commission.

†On leave of absence from the University of Louvain, Belgium.

Fermi interaction, i.e., a left-handed neutrino with a V and A interaction?

From the shape of the μ^+-decay spectrum we know that the μ^+-decay interaction is of the V and A type and that the neutral particles are distinguishable, i.e.,

$$\mu^+ \rightarrow e^+ + \nu + \tilde{\nu}. \qquad (1)$$

Therefore, the μ^+ is an antilepton (μ^+, e^+, and ν are antileptons). Then we can conclude from

$$\pi^+ \rightarrow \mu\mu^+ + \nu \qquad (2)$$

that the neutral particle is a neutrino.

Lee[5] gives a qualitative argument that relates the sign of the polarization of the μ^+ and the β particle, which is repeated here.

At the high-energy end of the beta spectrum the neutrino and antineutrino are emitted together in the opposite direction from the beta particle. Because the neutrino and antineutrino spin in opposite directions their net spin is zero, therefore the β particle has the same spin as the muon. From the asymmetry in the beta distribution it is known that those states are strongly favored in which the β-particle momentum is antiparallel to the muon momentum in the pion rest frame.[6] If the β particle is right-handed then the muon is left-handed, and vice versa. This result can be shown to hold for all electron energies, and the quantitative result is given in the comparison with the data in Section III D. Then it follows from Eq. (2) that the μ^+ is left-handed, and from Lee's argument that the high-energy e^+ is right-handed. Similarly the μ^- is right-handed and the high-energy e^- is left-handed.

Preliminary experimental results reported by Coffin et al.[7] disagree with the expected value. Their results were only tentative and subsequent results were inconclusive.[7]

We undertook a new experimental determination of the polarization for both the electron and the positron from μ decay. Meanwhile, Culligan et al. obtained a result for the positron polarization in agreement with the V-A interaction and left-handed neutrino.[8]

In this paper we present our results for both positron polarization and electron polarization in the μ decay.

The reversal of the sense of polarization of positron and electron is of interest both from experimental and from theoretical points of view.

1. Experimentally some of the systematic errors that may be present in this type of measurement will be eliminated if the magnitudes of the observed asymmetries are equal. The difference between the observed asymmetries is insensitive to errors, which are often difficult to eliminate with complete certainty.

2. It is frequently stated that the parity-nonconserving experiments have also demonstrated that charge-conjugation invariance is violated. Actually it is P and the product P T that are not conserved; therefore, either C or CPT is not conserved.[9] Since CPT invariance follows from extremely general principles, it would be difficult to accept a contrary result (i.e., that the sense of polarization was the same for both electrons and positrons) within the framework of the present theories. However, relatively independent of such theories, a change in sign of polarization for electron and positron coming via unpolarized muons from negative and positive pions clearly demonstrates the failure of the invariance of the weak decay processes under charge conjugation.

II. EXPERIMENTAL ARRANGEMENT AND METHOD

The technique used to determine the polarization of high-energy β particles from μ decay is an extension of that used by Goldhaber et al.[10, 11] It depends on two phenomena: (a) the bremsstrahlung radiation from a longitudinally polarized β ray is circularly polarized, and (b) the Compton transmission of circularly polarized γ rays through magnetized iron depends on the field direction and magnitude. As helicity is strongly conserved in the bremsstrahlung process, determining the direction of the polarization of circularly polarized γ rays also determines the direction of the β-ray polarization.

Beta particles from both μ^+ decay and μ^- decay were studied. The $\beta^\pm$ particles arose from decay at rest of $\mu^\pm$ mesons from a meson beam stopped in carbon. The μ^+ mesons are produced by the decay of stopped π^+; the μ^- by decay in flight of π^- mesons.

A. Meson Beam.

Mesons are produced by the 740-Mev circulating beam of the 184 inch synchrocyclotron striking a $\frac{1}{2}$-by-$\frac{1}{2}$-inch 2-inch-long beryllium target. These mesons are momentum-analyzed by the cyclotron field and then enter the magnetic channel shown in Fig. 1. The beam of positive mesons is monitored and degraded in energy in the range telescope before being brought to rest in a carbon stopper, which serves as the β-particle source.

A momentum of 210 ± 12 Mev/c was accepted by the magnetic channel. This channel consists of (a) a 24-inch-long quadrupole magnet set, placed between the cyclotron tank and the cyclotron shielding wall, (b) an 8-by-12-in 8-ft-long iron collimator through the shielddng wall, (c) a strong-focusing 30° bending magnet, (d) a second quadrupole pair mounted in a 4-ft-thick shielding wall, and (e) a 45° bending magnet.

Additional shielding was placed as shown between the counters and the cyclotron along the direction of spray from the cyclotron pole pieces.

The arrangement for monitoring and stopping the mesons is shown in Fig. 2. A 1-in-thick carbon slab was placed in front of the first counter to eliminate protons in the beam. The counters were 8-3/4 × 8-3/4 × 1/4-in plastic scintillator viewed by RCA-6810 A photomultipliers.

For the μ^+ experiment, π^+ mesons were brought to rest in the stopper. Pion decay at rest gives unpolarized muons.

In the μ^- experiment μ^-'s were stopped. These are obtained by reversing the cyclotron field and all the magnet fields, and using additional absorber. Then the μ^- (which have a longer range) are brought to rest in the carbon stopper. The μ^-'s are depolarized, owing both to the stopping material and to the cyclotron residual field of ~ 50 gauss present at the absorber.

The intensity of the π^+ beam, which comes off the target in the direction opposite to the bombarding protons, was $\sim 6 \times 10^6$ particles/minute. The π^- beam, which comes off in the forward direction, was ~3 times as intense, but because only 10% of this beam is μ^-'s, the rate for the μ^- experiment was less than half that for the μ^+ experiment. The range curve for the positive pion beam is shown in Fig. 3.

B. Polarization Analyzer

Figure 2 shows a scale sketch of the analyzer arrangement. A vertical alignment of the analyzer axis was chosen in order to remove the β and γ detectors from the plane of the meson beam and the median plane of the cyclotron. The β rays coming from the meson stopper are monitored by the β telescope.

The counters β_1, β_2, and β_3 are $\frac{1}{4}$-in-thick plastic scintillators viewed through 3-ft-long light pipes by RCA 6810A photomultipliers. Long light pipes were required to minimize the effect of the analyzer field on the sensitivity of the photomultiplier. Concentric soft iron and mu metal cylinders shield the phototube from the residual field. The β rays produce γ radiation in the target, in

the β_1 β_2 counters, and in the $\frac{1}{4}$-in. lead converter. The mixture of photons and electron-positrons strikes a 6-in.-thick iron cylinder magnetized to saturation, and those emerging are counted in the γ counter. A differential range curve of the stopping mesons obtained with the β_1 β_2 counters is given in Fig. 3.

The magnetized iron cylinder, 6 in. in diameter and 6 in. long, completed the magnetic circuit of an H-type magnet, which was driven near saturation by 30 amps through 500 turns. Figure 4 is a map of the field component in the z direction. The average field B_z is about 15.7 kilogauss for 6 in. Measurement of the photon circular polarization is made by registering the transmission through the iron when the magnetic field points toward the lead converter (up) and opposite to it (down).

A third counter (β_3) between the iron core and NaI crystal is used in part of the experiment to detect charged particles coming out of the iron.

The gamma radiation was detected by a NaI(Tl) Harshaw crystal, 4 in. in diameter and 4 in. thick, viewed by an RCA 6810A photomultiplier. The photomultiplier tube was shielded from the analyzer field by four concentric magnetic shields, two soft iron shields, and two mu metal shields. The energy determination is obtained from the amplitude of the signal taken from the fourth dynode. This output for an anode voltage of 1800 v is required to obtain linearity over the energy range we used; Fig. 5 shows the resolution measured for γ-ray energies of 1.16 and 1.33 Mev from Co^{60} and for 14.8- and 17.5-Mev γ rays resulting from the Li^7 (p, γ) Be^7 reaction using 450-kev protons. The energy scale is linear within 10% and the resolution has a full width at half maximum of $< 10\%$.

C. Electronics

The electronics shown in Fig. 6 consists of a ten-channel pulse-height analyzer gated by a β_1 β_2 γ (or β_1 β_2 β_3 γ) coincidence formed in a coincidence circuit with a resolving time of $\sim 2 \times 10^{-8}$ sec.

The pulse-height analyzer measured the amplitude of the signal from the fourth dynode of the NaI photomultiplier tube with an integrating time constant of several microseconds.

The β_1 β_2 coincidence rate was registered independently in a fast-counting channel and was used for relative normalization of the data. We also counted the number of γ rays (without the β_1 β_2 γ-coincidence gate requirement) with pulse

heights greater than the minimum analyzer channel. These counts, which were mainly background not associated with the β-γ events, provided us with a sensitive indicator for any small influence of the analyzer field on the γ detector.

The π_1-π_2 coincidence rate provided a continuous monitor on the meson beam, and an ionization chamber within the cyclotron vault monitored the cyclotron internal beam.

D. Operation and Calibration of Electronics

Photomultiplier voltages and coincidence discriminators were adjusted to optimize the signal-to-accidental ratio without sacrificing stability.

The β telescope was adjusted well up on its sensitivity plateau to reduce drift and minimize any changes in tube gain due to the analyzer fringe field.

The signals to the fast coincidence channel are voltage-limited before the coincidence requirement is met.

The pulse-height analyzer was calibrated with a Co^{60} source at regular intervals during the experiment and variations of the pulse height were less than 2%. We define the signal as the sum of the counts in the ten-channel pulse-height analyzer, and by accidentals we mean the corresponding sum when the γ channel has been delayed by 16×10^{-8} sec with respect to the β channel of the fast-coincidence circuit.

During most runs, the pulse-height analyzer channels, 3 Mev wide, covered energies from 2 to 28 Mev. Tables I and II show the signal and accidentals rates in different energy intervals for the experiments.

Some of the background in the pulse-height analyzer signal comes from accidental coincidences in the fast channel that opens the gate of the pulse-height analyzer. These are mainly accidentals between real β_1 β_2 events and random γ pulses, which are far more numerous when pulses are small than when they are large (as shown in Fig. 7).

The amplitude of the γ-ray signals (which is differentiated and used for the β β γ coincidence) is adjusted so that there will be reasonably high sensitivity over the entire pulse-height interval corresponding to 2-to-28-Mev γ-ray energies in the pulse-height analyzer. If the γ-ray sensitivity is set for too low a pulse-height amplitude the number of accidental gates increases rapidly. In practice the γ-ray sensitivity was adjusted for each run to give a satisfactory signal-to-accidental ratio in the 8-to-28-Mev region. This sometimes resulted in a loss of sensitivity in the lowest energy channel. The sensitivity for the low-energy channel varied from a minimum of ~30% to ~80%, depending on the shielding conditions, beam level, etc.

Table I. Data for various μ^+ mesons. (See text).
Numbers of events observed in each pulse-height channel

	e^+	Number of coincidences $\beta_1 \beta_2$ ($\times 10^6$)	Total time of observations Δt (min)	Number of γ rays ($\times$ 1024)	Channels (pulse energies, in Mev) 2 - 3	3 - 5	5 - 8	8 - 11	11 - 12	12 - 14	14 - 16	16-17	17 - 20	20 - 22	22 - 25	> 25
October Runs	Total Coinc. (↑)	324.4	646	9,654		242,915	95,354	12,986		5,612		5,347				
	Total Coinc. (↓)	324	641	9,519		233,093	92,646	12,237		5,260		5,048				
	Background (↑)	93.8				64,088	20,613	905		332		500				
	Background (↓)	93.6				65,698	19,795	893		333		463				
	δ (%)						+1.1 ± 2.8	+7.2 ± 2.0	+8.7 ± 2.9				+ 8.5 ± 3.7			
January Runs	Total Coinc. (↑)	176.1	438.9	2,352		17,627	5,963	4,272	1,784		1,196		1,207	740	652	794
	Total Coinc. (↓)	173.3[a]	439.7	2,297		16,621	5,804	4,002	1,582		1,146		1,104	686	570	744
	Background (↑)	53.4				1,826	512	320	42		37		41	30	45	110
	Background (↓)	53.1				1,642	474	346	48		24		32	20	45	92
	δ (%)					+1.6 ± 2.4	+3.2 ±3.3	6.3 ±2.4	+7.2 ± 3.0				+9.4 ± 3.4			
March Runs	Total Coinc. (↑)	396	604.4	2,841	20,735	31,641	15,546	6,664	3,212		2,830		2,179	1,000	540	570
	Total Coinc. (↓)	388.3[a]	588.9	2,751	20,417	30,136	14,729	6,215	2,969		2,569		2,116	937	474	662
	Background (↑)	77.9			1,595	2,274	323	58	27		24		34	22	27	
	Background (↓)	77.7			1,617	2,264	337	56	41		27		34	14	16	
	δ (%)				+2.53 ± 1.26		+ 3.83 ± 1.37	+5.23 ±1.89	+ 6.90 ± 2.0				+ 3.73 ± 2.8			
Total δ (%)				+0.63	+2.17 ± 1.01		+3.30 ± 1.15	+6.20 ±1.17	+ 7.30 ± 1.42				+ 6.64 ± 1.87			

[a] These runs were made with different weight; i.e., the accumulated charges on the beam integrator were unequal.

Table II. Data for various μ^- mesons (See text.)
Numbers of events observed in each pulse-height channel.

	e^-	Number of coincidences $\beta_1 \beta_2$ ($\times 10^6$)	Total time of observations Δt (min)	Number of γ rays ($\times$ 1024)	Channels (pulse energies, in Mev) 2 - 3	3 - 5	5 - 8	8 - 11	11 - 14	14 - 17	17 - 20	20 - 22	22 - 25	> 25
November	Total coinc. (↑)	353	610	1,236		78,989	22,147	4,721	1,842	1,384	1,048	1,741		986
	Total coinc. (↓)	368[a]	641	1,285		78,626	23,681	5,296	2,215	1,469	1,073	1,851		986
	Background (↑)	155				28,300	4,560	770	427	395	351	584		369
	Background (↓)	171[a]				29,302	5,094	811	465	442	384	596		394
	δ (%)						-4.84 ±2.13	-13.18 ± 3.38			-1.30 ± 7.55			
January	Total coinc. (↑)	147.5	862	7,204	106	831	1,659	1,393	761	789	655	501	560	1,227
	Total coinc. (↓)	148.7	865	7,134	94	736	1,582	1,401	779	812	703	514	572	1,286
	Background (↑)	15.7			4	27	37	4	3	1	5	8	5	16
	Background (↓)	15.7			3	22	34	6	2	3	2	6	7	29
	δ (%)					+10.5 ± 5.6		-0.91 ± 2.85			- 3.65 ± 4.31			
February	Total coinc. (↑)	154.9	671	6,525	2,137	11,492	4,811	1,956	960	793	681	340	348	685
	Total coinc. (↓)	155.2	662	6,418	2,339	11,159	4,865	1,824	992	756	745	336	378	764
	Background (↑)	38.6			127	1,366	304	38	19	28	35	37	44	65
	Background (↓)	37.2			152	1,246	276	43	27	26	44	34	53	71
	1 (%)					+ 3.28 ± 2.59		+ 4.88 ± 3.15			-9.61 ± 7.7			
March	Total coinc. (↑)	147.6	245	2,413	1,414	11,549	3,562	1,242	627	579	516	315	326	640
	Total coinc. (↓)	147.6	243	2,377	1,386	11,233	3,561	1,316	633	667	537	306	349	643
	Background (↑)	28.8			121	1,220	176	28	14	23	24	20	17	80
	Background (↓)	23.9[a]			78	961	134	19	17	14	15	12	36	69
						+3.91 ± 2.78		-7.6 ± 3.58			-4.31 ± 7.5			
	δ (%)			+ 1.65		+0.91 ± 1.37		-3.71 ± 1.61			-4.28 ± 3.10			

[a] These runs were made with different weight; i.e., the accumulated charges on the beam integrator were unequal.

E. Experimental Procedure

To cancel out any effects due to equipment drift or variations in the operation of the cyclotron, we made alternate runs of about 10 minutes each, first with the field up (toward the lead radiator) then with the field down. The length of the run was determined by the accumulated charge from an ionization chamber placed near the meson port of the cyclotron. Measurements were made to show that runs of equal accumulated charge produced the same total number of $\beta_1 \beta_2$ coincidences over a change of at least a factor of 10 in the $\beta_1 \beta_2$ rate. "Accidentals" runs with field up and field down were taken about every fifth cycle.

III. RESULTS AND DISCUSSION

A. Data

The data taken over several days' running time were reduced as follows: (a) The numbers of $\beta_1 \beta_2$ coincidences and counts in each channel of the pulse-height analyzer were added together for all runs with field up and with field down, (b) The totals for field down were normalized to the same total number of $\beta_1 \beta_2$ coincidences as with field up, (c) All accidentals-measuring runs (field up and down) were totaled together and normalized in the same way. Then the quantities we call $N_i(\uparrow)$ and $N_i(\downarrow)$ (where i is the channel number) are obtained by subtracting accidental counts from the signal.

Table I and II show the data for each run.

Figure 8 shows the pulse-height spectrum for the γ rays with the 6 in. of iron in place. The central curve $\beta_1 \beta_2 \gamma$ is our main signal.

The variable δ used to interpret the result of these experiments is derived from the experimentally measured quantities by the formula[12]

$$\delta_i = [N_i(\uparrow) - N_i(\downarrow)] \,/\, \tfrac{1}{2}[N_i(\uparrow) + N_i(\downarrow)] \,. \qquad (3)$$

Figure 9 shows a plot of δ, where different energy channels have been grouped together so that each group has roughly the same net number of counts in it, the errors shown are based on the counting statistics only.

The numbers indicated in the figure have been corrected from Tables I and II for a small shift in the zero. (See Section III B.)

B. False Asymmetry Due to Field Dependence of the γ-Ray Counter

Examination of Tables I and II shows that the number of ungated γ rays with pulse heights greater than the minimum analyzer channel (γ) was consistently larger with field up than with field down for both e^+ and e^- runs. In fact, there was an asymmetry of +1.5% when all runs were averaged. We believed this effect was due to magnetic-field effect on the photomultiplier sensitivity. To test this hypothesis we went to a different geometry where we computed the instrumental asymmetry and then checked it by a direct measurement of the asymmetry.

Figure 4 shows the field distribution for two different geometries. On the left side is the "usual geometry" used for the polarization measurements, while on the right side is the "hollow geometry" used to check instrumental asymmetries. In the hollow geometry the excitation of the analyzer magnet produces approximately the same field at the photomultipliers as the usual geometry, but with only 2 inches of magnetized iron in the path of the γ rays. As a result, owing to the reduced length of the magnetized iron the residual asymmetry was about 10% of that for the usual geometry, i.e., instead of 3.5% to 6.3% the residual asymmetry is 0.35% to 0.63% for 100% polarized β rays.

To simulate the kind of asymmetry introduced by a magnetic field effect on the NaI photomultiplier sensitivity we attenuated the γ-ray signal amplitude. We experimentally determined the curve δ (E),

$$\delta(E_i) = (N_i - N_i')/\tfrac{1}{2}(N_i + N_i'), \qquad (4)$$

where N_i and N_i' represent the numbers registered in channel "i" without and with attenuation. The attenuation factor was adjusted to give the same average asymmetry in the ungated γ-ray channel as that produced by reversing the magnetic field direction. This δ(E) curve is reported in Fig. 10 (Curve b). We see that, combining it with the hollow geometry (Curve a for right helicity, Curve c for left helicity), we are able to explain within statistical accuracies the origin of the experimental points found with this geometry. Therefore, we use the same procedure to calculate the known instrumental asymmetry in the "usual geometry."

Owing to the existence of this instrumental asymmetry it probably would have been desirable to further improve the magnetic shielding of the γ counter. However, we chose to stop when this asymmetry was of the order of the

statistical limits. In fact, the procedure used to correct the asymmetries introduces an error that can be neglected. The whole effect is sufficiently small so that, for example, one might assign a constant zero shift of 1.5% to the empirical result in Tables I and II. If one applies this directly to the result in Fig. 9, the agreement between the points and the curve is perhaps even better. However, to justify the constant-shift procedure one would have to assume a different (but as yet unidentified) source of the false asymmetry.

C. Enumeration of Possible Sources of Asymmetries

Before comparing the observed results with the theory we will describe some of the sources of asymmetries that come from spurious effects. We will divide these effects into two classes. Class A effects are in the same direction for either plus or minus muons. Class B effects reverse with change in sign of the particle being studied; that is, they behave in the same way as the signal.

Class A: Sign of Asymmetry Independent of Sign of Particles

1. Field effects on the gamma counter

The one effect that we are sure is present is associated with the fringe field of the analyzer magnet on the γ-ray counter. The lack of cylindrical symmetry in the phototube construction gives rise to different sensitivities for small fields in different directions. The size of the effect is due to the combination of the cyclotron fringe field with the analyzer field so that it is not necessarily of the same magnitude when the cyclotron field is reversed.

2. Field effects on the beta counter

The β counters also are sensitive to the fringe field of the analyzer. It was found that the only positive way to eliminate these effects was to add a 3-ft light pipe on these counters. In the final geometry, less than 10 gauss was present at the exterior of the magnetic shield and no asymmetry in β counts was seen (to an accuracy of ~1%), as shown in Tables I and II.

3. Compton component in the shower

The shower that develops in the iron includes Compton-scattered electrons. If these electrons are deflected by the field of the analyzer in such a way as to increase (or decrease) the transmission through the iron, the effect will be the same for both signs of mu mesons. We believe that such an effect is eliminated by the geometrical symmetry of the detection system, as discussed directly below.

Class B: Sign of Asymmetry Dependent on Sign of Particles

1. Deflection of the Shower Particles

Orbits of the shower particles excluding the Compton-scattered component are deflected by the magnetic field. When the sign of the primary β particles is changed the orbits of the shower particles are then interchanged, i.e., field-up orbits for positrons are the same as field-down orbits for electrons. If the detector or the source is located on the axis of the analyzer the deflections with field up and with field down are mirror images. Therefore any decrease (or increase) in transmission is the same for the same magnitude of field. If the centers of the source and of the detector can be connected by a line that passes through the center of the analyzer, the same argument applies. The only geometric case for which there can be an asymmetry is that where in both source and detector are off the axis of symmetry of the analyzer, and then only the components separated by 90° in azimuth are affected. In our geometry the analyzer is built with an axis of symmetry and the detector is on the axis. The source is broadly illuminated and centered on the axis. The radiator is also located on the axis.

One would expect that such orbit effects would persist and be exaggerated in the lowest-energy gamma channels. No such effect is indicated in the data.

It does not appear to us that there are any orbit effects of a size comparable to the effects being observed here.

2. Compton component in the detector

Another method for measuring the polarization of γ rays is to measure a change in the yield of Compton electrons from magnetized iron. If the attenuation of Compton electrons is small this asymmetry is in the opposite sense from the absorption technique used here. To eliminate the possibility that our asymmetry might be cancelled or reversed by such processes, we performed an experiment more sensitive to this effect. In Fig. 2 the counter No. β_3 was added to detect those events with a charged particle leaving the iron absorber. The spectrum in Fig. 8 shows that the fraction of these events falls off toward low-energy γ rays, varying from 10% at the upper end to 3% at the lowest energy, and the asymmetry was measured with this as a signal. The results were in the same direction as the usual asymmetry. The Compton yield would drop off at higher pulse heights in the detecting NaI counter. We conclude that the largest fraction of these events is pairs made immediately before the detector, and their asymmetry would not be distinguishable from the parent γ rays.

D. Comparison with Theory

The spectrum for μ decay[1, 2, 11] with the two-component theory is given as

$$N(x)\,dx\,d\Omega = 2x^2\,[3 - 2x \pm \{\xi(1 - 2x)\cos\theta\}]\,(dx\,d\Omega)/4\pi$$

where $x = E/W$, W is the maximum energy of the spectrum $(\sim M\mu c^2/2) = 52.8$ Mev,

$$\xi = \frac{g_V g_A^* + g_V^* g_A}{|g_V|^2 + |g_A|^2} ,$$

and θ is the angle between the electron momentum and the μ spin. The polarization of the electrons for the parallel and antiparallel unpolarized muons is

$$\frac{N_p}{N_a} = \frac{|g_V - g_A|^2}{|g_V + g_A|^2} = \frac{1 - \xi}{1 + \xi} .$$

The ξ parameter has been estimated from the asymmetry experiments,[13]

$$|R\,\xi| = 0.87 \pm 0.12 ,$$

where R represents the depolarizing effects, polarization of muon beam, etc.

The percent of polarization of the electrons is

$$\left|\frac{N_a - N_p}{N_a + N_p}\right| = \xi \geqslant 0.87.$$

Therefore within the two-component theory the asymmetry experiments establish a lower limit of 0.74 for the polarization. Clearly to improve this limit requires a measurement of accuracy better than 10%, which it will be seen is not possible at this stage by this experiment. The polarization has been calculated by Kinoshita and Sirlin[11] for the four-component theory. There are, however, no restrictions on the polarization. The relation between the polarization of the $\pi^+ - \mu^+$ decay and $\pi^- - \mu^-$ decay was shown to be a consequence of the CPT theorem.[9, 11]

The scattering of circularly polarized photons by an electron with its spin polarized along the photon direction has a cross section

$$\sigma = \sigma_0 \pm \sigma_1 ,$$

where the positive sign refers to photon spin along its momentum,

$$\sigma_1 = \frac{4}{3}\,\sigma_T \left[\frac{1 + 4\gamma + 5\gamma^2}{\gamma\,(1+2\gamma)^2} - \frac{1+\gamma}{2\gamma^2}\,\ln\,(1 + 2\gamma)\right] ,$$

σ_0 is the non-spin-dependent total Compton cross section, σ_T is the Thomspon cross section, and $\gamma = E_\gamma / m_e c^2$ is the initial gamma energy in electron rest-mass units.[14]

In the attenuation of a line spectrum for good geometry, the asymmetry for the transmitted intensity, with iron of length L in which $\bar{\nu}$ electrons per atom are polarized along or against the photon direction, is

$$\delta = \mp\ 2 \tan L\,(N\,\bar{\nu}\,\sigma_1\,L)$$

where the negative sign refers to a photon with its spin along its momentum, N is the number of atoms per unit volume,

$$\bar{\nu} = \nu_0 \cdot \frac{(\overline{B - H})}{B_0} .$$

$\nu_0 = 2.02$ at room temperature, and $B_0 \sim 21.4$ kg.[15]

The polarization of the shower incident on the analyzer is not known. If we assume the McVoy and Dyson cross sections[16] we find that for a 100% forward polarization electron, the polarization P of the photons with an energy $k = \eta E_\beta$ is

$$P = \frac{N_{forward} - N_{backward}}{N_{forward} + N_{backward}} = \left(\frac{\eta - {}^2/4}{1 - \eta + 3\eta^2/4}\right) .$$

We have calculated polarization for photons produced by the bremsstrahlung of the μ-decay beta particles, including the energy loss up to the beginning of the radiator. If we assume that the radiator is thin and neglect the shower in the radiator and the iron, we obtain as estimates for the photon polarization the values given in Table III.

A calculated spectrum (summed over the γ polarization after passing through the 6 inches of iron) is given in Fig. 8, corrected only for attenuation. At low energy this spectrum appears to be low, presumably owing to neglect of the cascade effects.

The actual polarization will be different from this simple model, and work is in progress on a detailed calculation of such cascade effects.[17] It does not seem unreasonable to us that in the cascade shower for photons near the critical energy (7 Mev in lead), the polarization might be strongly enhanced over that calculat

The preliminary Monte Carlo results for the γ-ray polarization obtained by Cook and Williams[17] for a shower made in 0.5 cm of lead by 30-Mev electrons already indicate several points.

(a) The polarization below 5 Mev follows the McVoy-Dyson result and is approaching zero as indicated in Fig. 9.

(b) Above 15 Mev there were no backwards photons and 46 forward photons (500 incident electrons were followed).

(c) In the region between 5 and 20 Mev the statistics are not sufficient to establish any deviation from the McVoy-Dyson results.

These results as applied to this work can be interpreted as follows. The McVoy-Dyson polarization is a good approximation to the actual polarization, although for photons with energy of about one-half the incident energy, the indication is that it underestimates the polarization.

To obtain an upper limit for the asymmetry measurement, we can assume 100% polarization. This is plotted in Fig. 9.

TABLE III. Calculated asymmetries: δ_I is calculated on the assumption of good geometry. P is the gamma-ray polarization calculated by using the McVoy-Dyson results, and δ_{II} is the expected asymmetry with this assumption. The measured asymmetry is expected to fall between these two results.

E (Mev)	2.5	5.0	10	15	20	25
δ_I	9.3	9.0	7.2	6.0	5.1	4.5
P	12	24	45	64	78	88
δ_{II}	1.1	2.2	3.2	3.8	4.0	4.0

In order to obtain a best value for the observed asymmetry, we must combine the data, correcting for the known instrumental asymmetries. We have done so in Table IV for both charged muons. The γ-ray energy is cut off at 8 Mev to reduce the uncertainties in the expected asymmetry due to possible shower effects.

TABLE IV. Results combined for γ-ray energies greater than 8 Mev.

Particle	δ	Zero correction	Corrected δ	Calculated asymmetries
e^+	6.6 ± 0.8	+ 0.5 ± 0.2	+6.1 ± 0.9	+ 3.5 < δ < +6.3 (R. H.)
e^-	-3.9 ± 1.4	+ 1.0 ± 0.4	-4.9 ± 1.5	- 6.3 < δ < -3.5 (L. H.)
combined	$\lvert\delta\rvert$ = 5.8 ± 0.7			
calculated	δ 3.5 < $\lvert\delta\rvert$ < 6.3			

IV. CONCLUSIONS

The results, as shown in Table IV and Fig. 9 indicate that β^+ is right-handed and β^- is left-handed. For the two-component theory, μ^+ is left-handed, and μ^- is right-handed.[18] The results are in agreement (or, more accurately, not in disagreement) with the assumption of (a) the two-component theory with left-handed neutrinos, (b) conservation of leptons, (c) universal β-decay theory with V and A interactions, (d) complete polarization of both β^+ and β^-.

ACKNOWLEDGMENTS

We wish to thank Gordon M. Bingham, John F. Kenney, Hans W. Kruger, and Ralph Nobles for assistance in setting up the apparatus and taking the data and James Vale, Lloyd Houser, and members of the cyclotron crew for providing many hours of steady beam. We should like to express appreciation to Drs. Sidney A. Bludman, Maurice Goldhaber, Leon M. Lederman, Edwin M. McMillan, and Robert L. Thornton for the valuable criticism and encouragement they gave during the course of the work.

One of us (P. C. M.) would like to acknowledge gratitude to the Institut Interuniversitaire des Sciences Nucléaires (Belgium) for the fellowship he received, and to all the people he worked with in the Radiation Laboratory for their friendship.

REFERENCES

1. T. D. Lee and C. N. Yang, Phys. Rev. 104, 254 (1956).
2. L. Landau, Nuclear Phys. 3, 127 (1957); T. D. Lee and C. N. Yang, Phys. Rev. 105, 1671 (1957); A. Salam, Nuovo cimento 5, 299 (1957).
3. See, for example, the general bibliography given by M. Gell-Mann and A. Rosenfeld, Ann. Rev. Nuclear Sci. 7, 407 (1957).
4. M. Goldhaber, L. Grodzins, and A. W. Sunyar, Phys. Rev. 109, 1015 (1958).
5. T. D. Lee, Proceedings of the Seventh Annual Rochester Conference on High-Energy Physics (Interscience, New York, 1957), p. VII-6.
6. R. L. Garwin, L. M. Lederman, and M. Weinrich, Phys. Rev. 105, 1415 (1957); J. I. Friedman and V. L. Telegdi, Phys. Rev. 106, 1290 (1957).
7. T. Coffin, D. Berley, R. L. Garwin, M. Weinrich, and L. M. Lederman, work reported by Lederman in Proceedings of the Seventh Annual Rochester Conference on High-Energy Physics (Interscience, New York 1957), p. VII-31; R. L. Garwin, Bull. Am. Phys. Soc. Ser. II, 2, 206 (1957); L. M. Lederman, private communication. We wish to thank Dr. Lederman for informing us of the progress of this work.
8. G. Culligan, S. F. Franck, J. R. Holt, J. C. Kluyver, and T. Massam, Nature 180, 751 (1957).
9. H. P. Stapp, Phys. Rev. 107, 635 (1957). We wish to thank Dr. Stapp for clarifying this point.
10. M. Goldhaber, L. Grodzins, A. W. Sunyar, Phys. Rev. 106, 826 (1957).
11. T. Kinoshita and A. Sirlin, Phys. Rev. 106, 1110 (1957), 108, 844 (1957); H. Uberall, Nuovo cimento 6, 376 (1957); C. Fransdale and H. Uberall, Nuovo cimento 8, 1091 (1958); C. Bouchiat and L. Michel Phys. Rev. 106, 170 (1957).
12. The convention here is that used in References 7, 8, 10, etc. For 100% polarization asymmetry we have $\delta = 2$.
13. D. H. Wilkinson, Nuovo cimento 6, 516 (1957).
14. S. B. Gunst and L. A. Page, Phys. Rev. 92, 970 (1957).
15. C. Kittel, Introduction to Solid State Physics (Wiley, New York, 1953), p. 166.
16. K. W. McVoy and F. J. Dyson, Phys. Rev. 106, 1360 (1957); K. W. McVoy, Phys. Rev. 106, 828 (1957).
17. L. F. Cook, Jr., and N. A. Williams, Jr., Polarization Effects in Cascade Showers, UCRL-8399, July 29, 1958.

18. The sense of asymmetry for μ^- decay is known from counter data only. One assumes that the polarizing mechanism--decay in flight--is the same for μ^+ and μ^-. The pion spectrum is of course different although Telegdi reported no change in the μ^- asymmetry coefficient for different pion-energy beams [Proceedings of the Seventh Annual Rochester Conference on High-Energy Physics (Interscience, New York, 1957), p. VII-33].

FIGURE CAPTIONS

Fig. 1. Plan view of the 184-inch cyclotron meson-beam facility. Beams of π^- mesons are obtained by reversing the cyclotron field and the beam-forming magnets.

Fig. 2. Details of the analyzer. π^+ (or μ^-) mesons stop in the tilted carbon stopper.

Fig. 3. Range curves for the π^+ beam. The π^+ rate and β^+ rate are in the same units plotted on different scales.

Fig. 4. The analyzer magnet core, showing at the upper left the configuration of iron. The lower left shows the measured field distribution. The upper right shows the "hollow geometry" and the lower right shows the field in this geometry.

Fig. 5. The pulse-height spectrum observed for Co^{60} gamma rays and $Li(p\gamma)Be^7$ gamma rays. The background for the Li γ rays has not been subtracted. The pulse-height channel numbers are proportional to the voltage. The arrows on the pulse-height scale indicate the expected positions of the gamma-ray peaks.

Fig. 6. The electronic block diagram, consisting of the π telescope (lower left) and the β telescope (upper half) of the fast-coincidence circuit. The $\beta_1\ \beta_2\ (\beta_3)\ \gamma$ coincidence (center) gates the γ-pulse-height analyzer.

Fig. 7. The γ background present in the μ^+ experiment. Notice the rapid variation between 5 and 10 Mev. Also shown is the accidental spectrum gates by delaying the γ pulse in the 10^{-8} sec coincidence circuit. There is no evidence of any γ pile-up in the slow-γ channels.

Fig. 8. The observed spectra of pulse heights for $\mu^+ \rightarrow \beta \rightarrow \gamma$ events. The $\beta_1\ \beta_2\ \gamma$ curve (top) shows the spectrum on which the asymmetry measurements are based. The $\beta_1\ \beta_2\ \beta_3\ \gamma$ spectrum (bottom) shows the relative sizes of events in which a β particle leaves the iron absorber. The dashed curve is the gamma-ray intensity calculated at the counter (cascade effects in the lead and iron neglected). For the transmission in the iron the total γ-absorption cross section is used.

Fig. 9. Asymmetry measurements obtained for β's from μ^+ and μ^- decay. The data have been corrected for a measured shift in the zero line due to the influence of analyzer magnetic field on the γ counter. The curves are calculated asymmetries; δ_I would be expected for 100% polarized photons, δ_{II} is calculated by assuming 100% polarized electrons make

bremstrahlung in the lead radiator but by neglecting multiplicative shower effects. The top curves are for right-handed particles and the bottom curves for left-handed ones. To change the assignment of the left- and right-handedness it would be necessary to reflect both expected curves above the zero line.

Fig. 10. Asymmetry measurements made with the "hollow" geometry of Fig. 4. The curves a and c reflect the small expected asymmetry due to the 2 in. of partially magnetized iron. The curve b represents the asymmetry expected due to the residual analyzer field on the γ counter for unpolarized gamma rays. The zero shift as applied to Fig. 9--the asymmetry results--is somewhat smaller ($\times$ 2/3) than the b curve for positive particles and 1/3 as large for negative particles.

Information Division
br

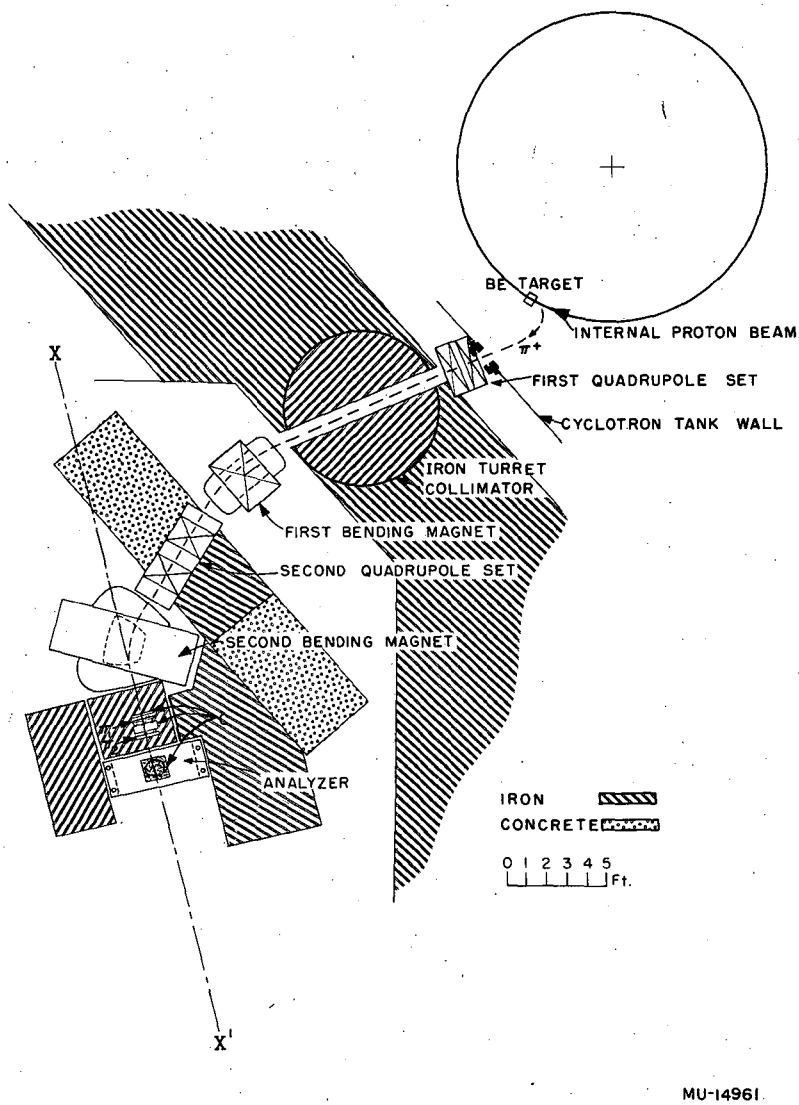
BE TARGET
INTERNAL PROTON BEAM
π^+
FIRST QUADRUPOLE SET
CYCLOTRON TANK WALL
IRON TURRET
COLLIMATOR
FIRST BENDING MAGNET
SECOND QUADRUPOLE SET
SECOND BENDING MAGNET
ANALYZER
X
X'
IRON
CONCRETE
0 1 2 3 4 5
Ft.
MU-14961

Fig. 1.

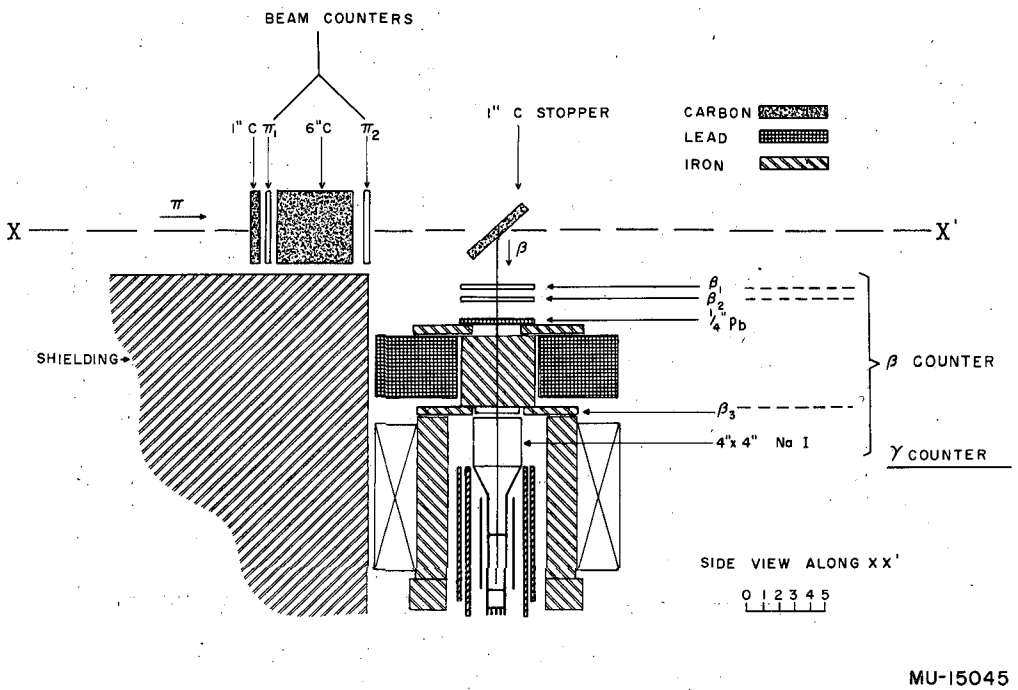
BEAM COUNTERS
1" C
π_1
6" C
π_2
1" C STOPPER
CARBON
LEAD
IRON
π
X
X'
β
β_1
β_2
1/4" Pb
SHIELDING
β COUNTER
β_3
4"x 4" Na I
γ COUNTER
SIDE VIEW ALONG XX'
0 1 2 3 4 5
MU-15045

Fig. 2.

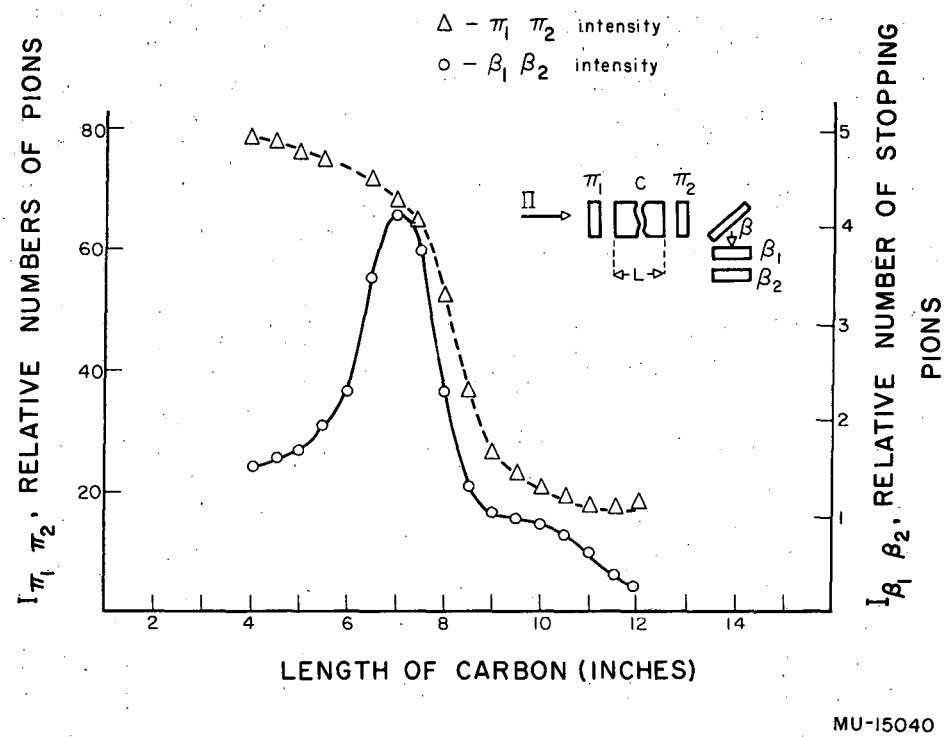
Δ – π_1 π_2 intensity
o – β_1 β_2 intensity
$I_{\pi_1 \pi_2}$, RELATIVE NUMBERS OF PIONS
$I_{\beta_1 \beta_2}$, RELATIVE NUMBER OF STOPPING PIONS
LENGTH OF CARBON (INCHES)
80
60
40
20
5
4
3
2
1
2
4
6
8
10
12
14
Π
π_1
C
π_2
L
β
β_1
β_2
MU-15040

Fig. 3.

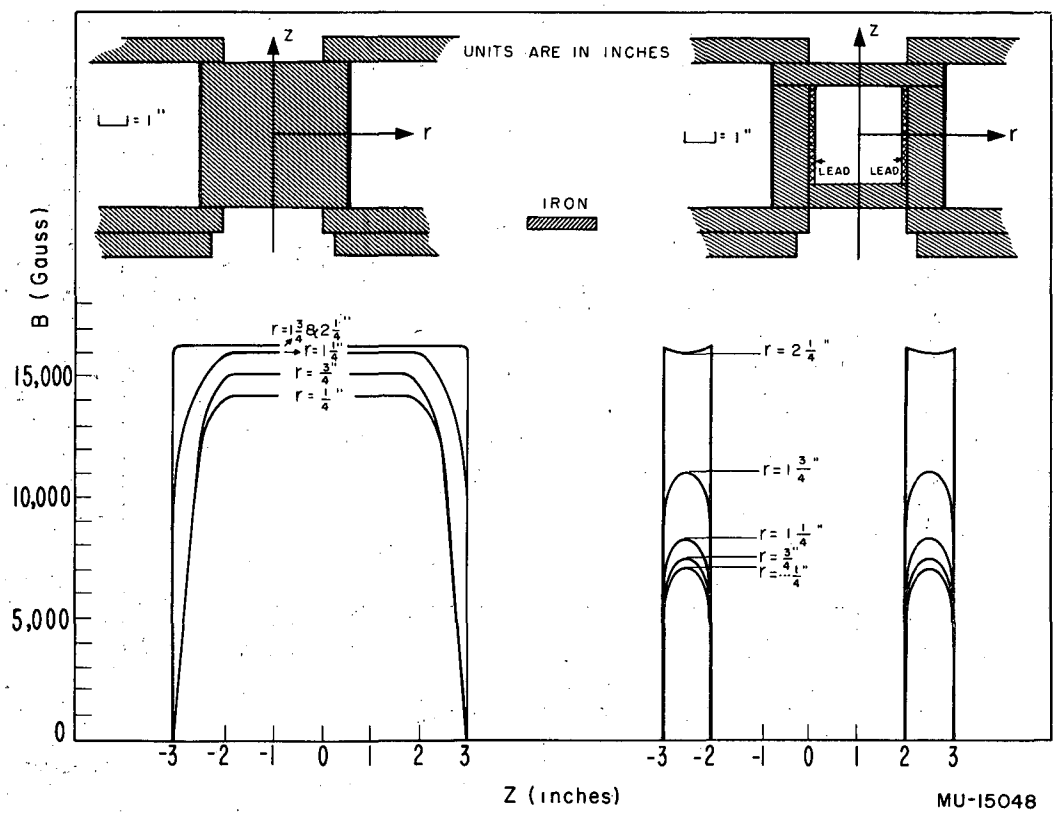
UNITS ARE IN INCHES
Z
r
= 1"
IRON
LEAD
LEAD
B (Gauss)
15,000
10,000
5,000
0
r = 1 3/4 & 2 1/4"
r = 1 1/4"
r = 3/4"
r = 1/4"
r = 2 1/4"
r = 1 3/4"
r = 1 1/4"
r = 3/4"
r = 1/4"
-3 -2 -1 0 1 2 3
Z (inches)
MU-15048

Fig. 4.

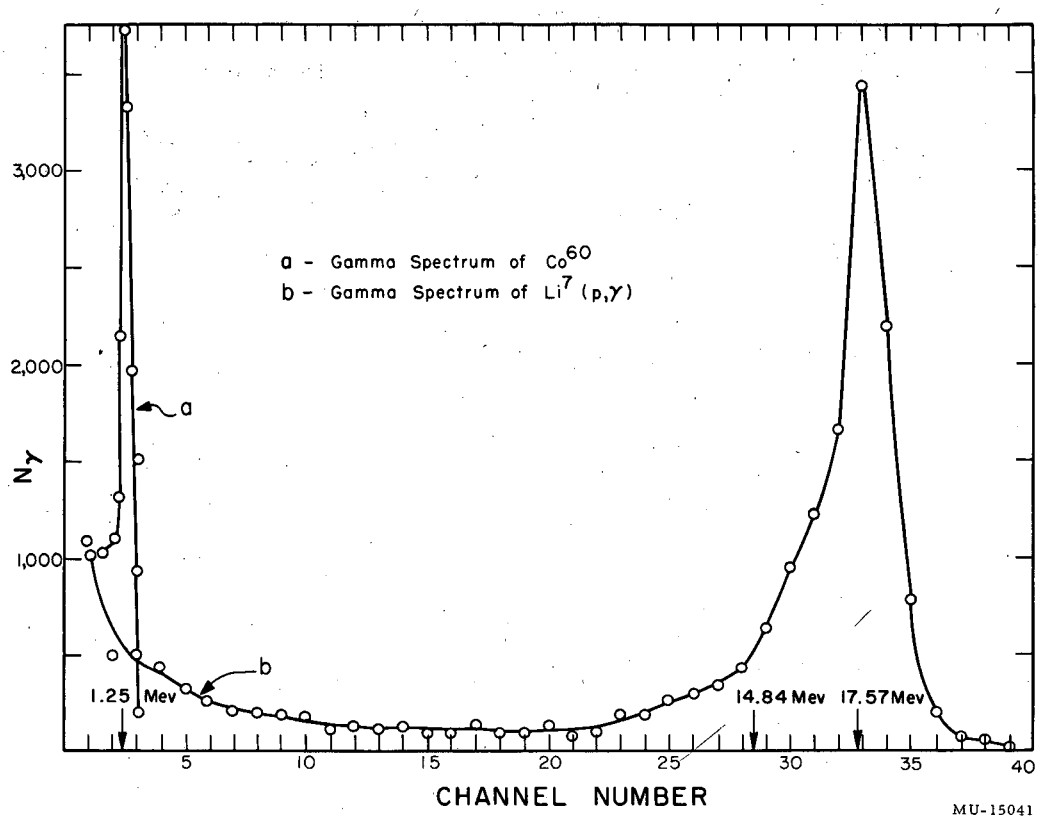
a - Gamma Spectrum of Co60
b - Gamma Spectrum of Li7 (p,γ)
3,000
2,000
1,000
Nγ
a
b
1.25 Mev
14.84 Mev
17.57 Mev
5
10
15
20
25
30
35
40
CHANNEL NUMBER
MU-15041

Fig. 5.

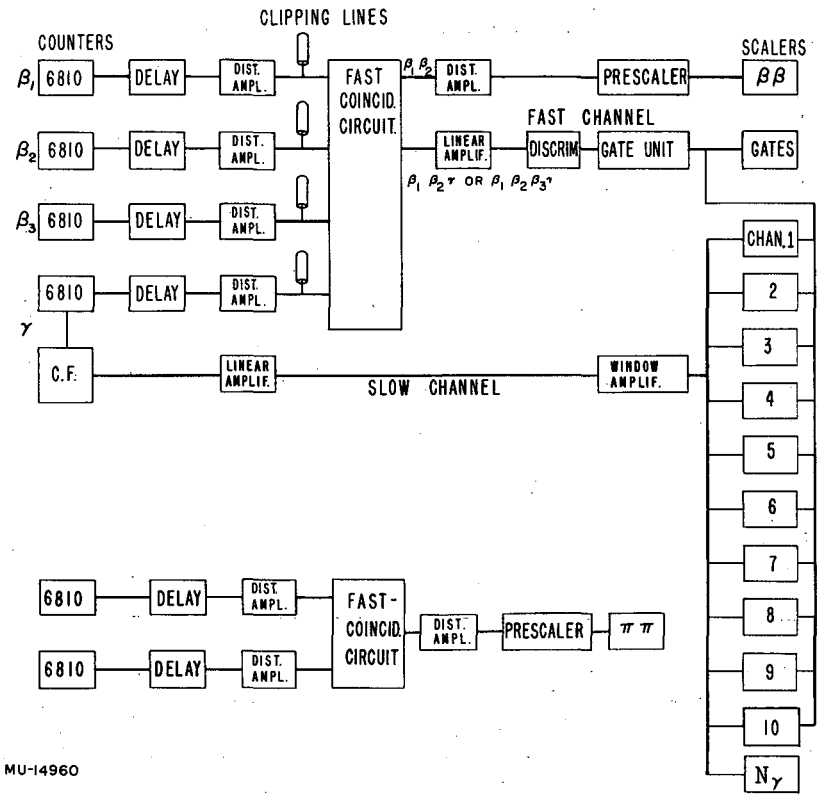
CLIPPING LINES
COUNTERS
SCALERS
β_1
6810
DELAY
DIST. AMPL.
FAST COINCID. CIRCUIT.
$\beta_1 \beta_2$
DIST. AMPL.
PRESCALER
$\beta\beta$
FAST CHANNEL
β_2
6810
DELAY
DIST. AMPL.
LINEAR AMPLIF.
DISCRIM
GATE UNIT
GATES
$\beta_1 \beta_2 \gamma$ OR $\beta_1 \beta_2 \beta_3 \gamma$
β_3
6810
DELAY
DIST. AMPL.
CHAN. 1
6810
DELAY
DIST. AMPL.
2
γ
3
C.F.
LINEAR AMPLIF.
SLOW CHANNEL
WINDOW AMPLIF.
4
5
6
7
6810
DELAY
DIST. AMPL.
FAST-COINCID. CIRCUIT
DIST. AMPL.
PRESCALER
$\pi\pi$
8
6810
DELAY
DIST. AMPL.
9
10
N_γ
MU-14960

Fig. 6.

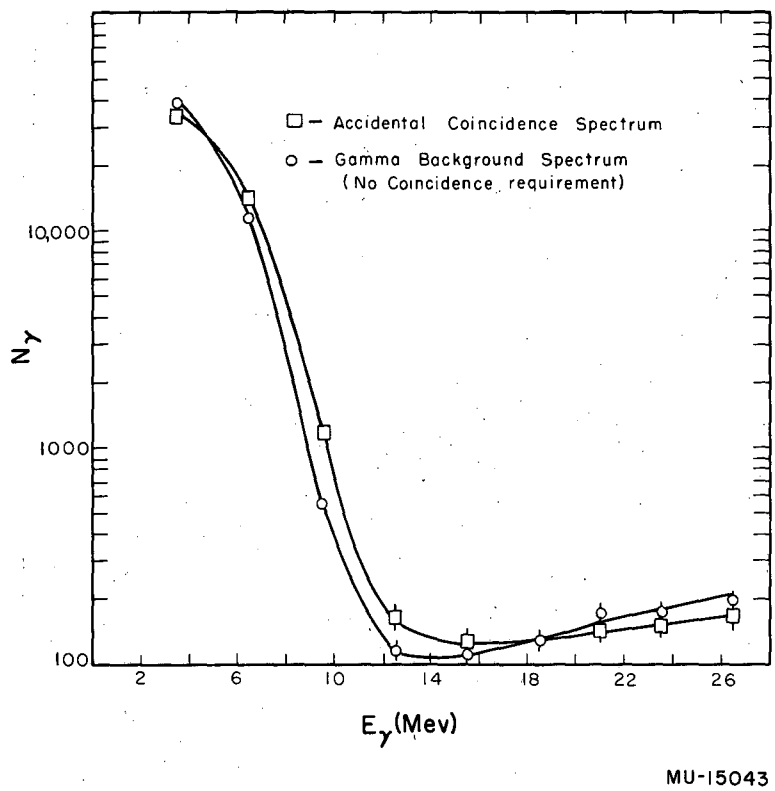
□ — Accidental Coincidence Spectrum
○ — Gamma Background Spectrum
(No Coincidence requirement)
10,000
1000
100
N_γ
2
6
10
14
18
22
26
E_γ(Mev)
MU-15043

Fig. 7.

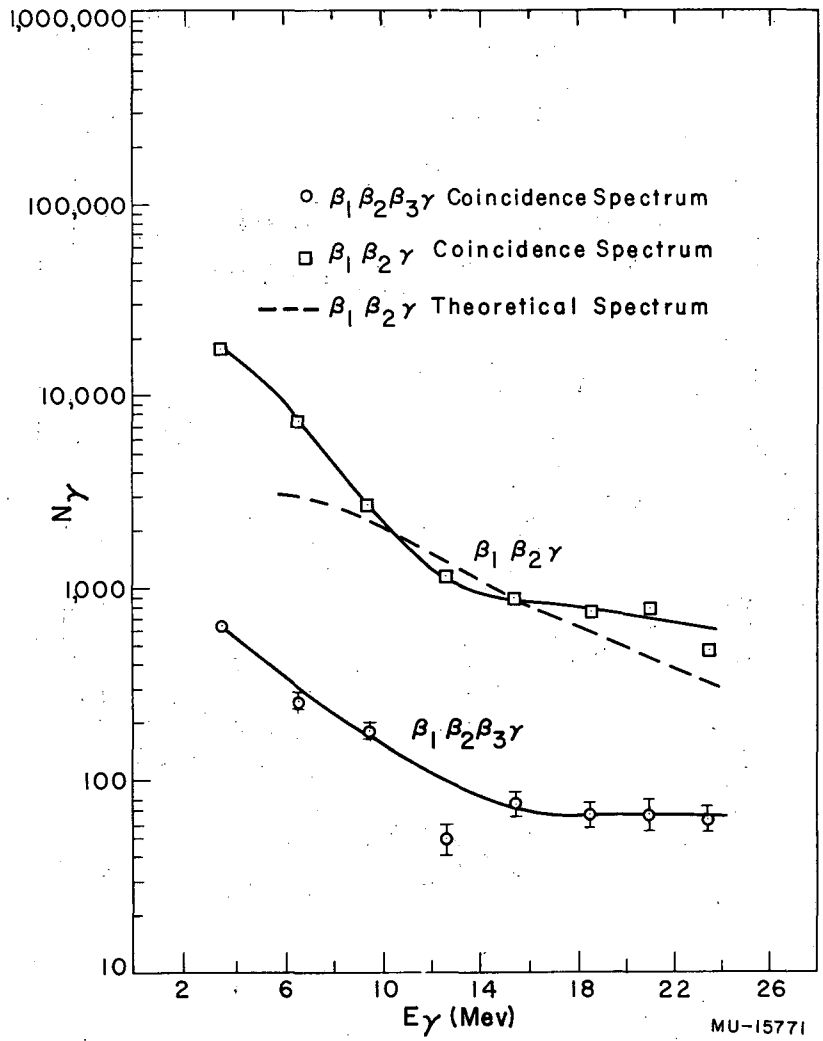
1,000,000
100,000
10,000
1,000
100
10
N_γ
○ $\beta_1 \beta_2 \beta_3 \gamma$ Coincidence Spectrum
□ $\beta_1 \beta_2 \gamma$ Coincidence Spectrum
--- $\beta_1 \beta_2 \gamma$ Theoretical Spectrum
$\beta_1 \beta_2 \gamma$
$\beta_1 \beta_2 \beta_3 \gamma$
2
6
10
14
18
22
26
E_γ (Mev)
MU-15771

Fig. 8.

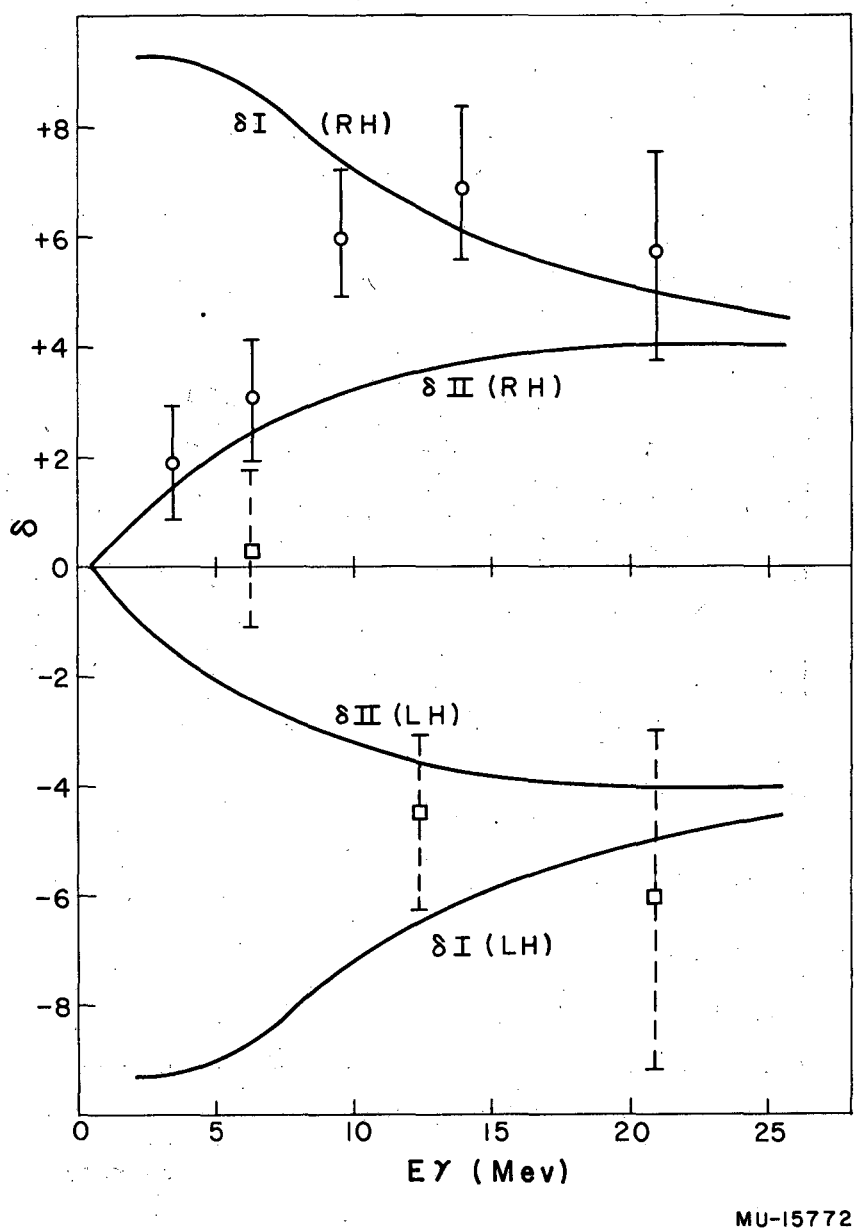
δI (RH)
δII (RH)
δII (LH)
δI (LH)
+8
+6
+4
+2
0
-2
-4
-6
-8
δ
0
5
10
15
20
25
Eγ (Mev)
MU-15772

Fig. 9.

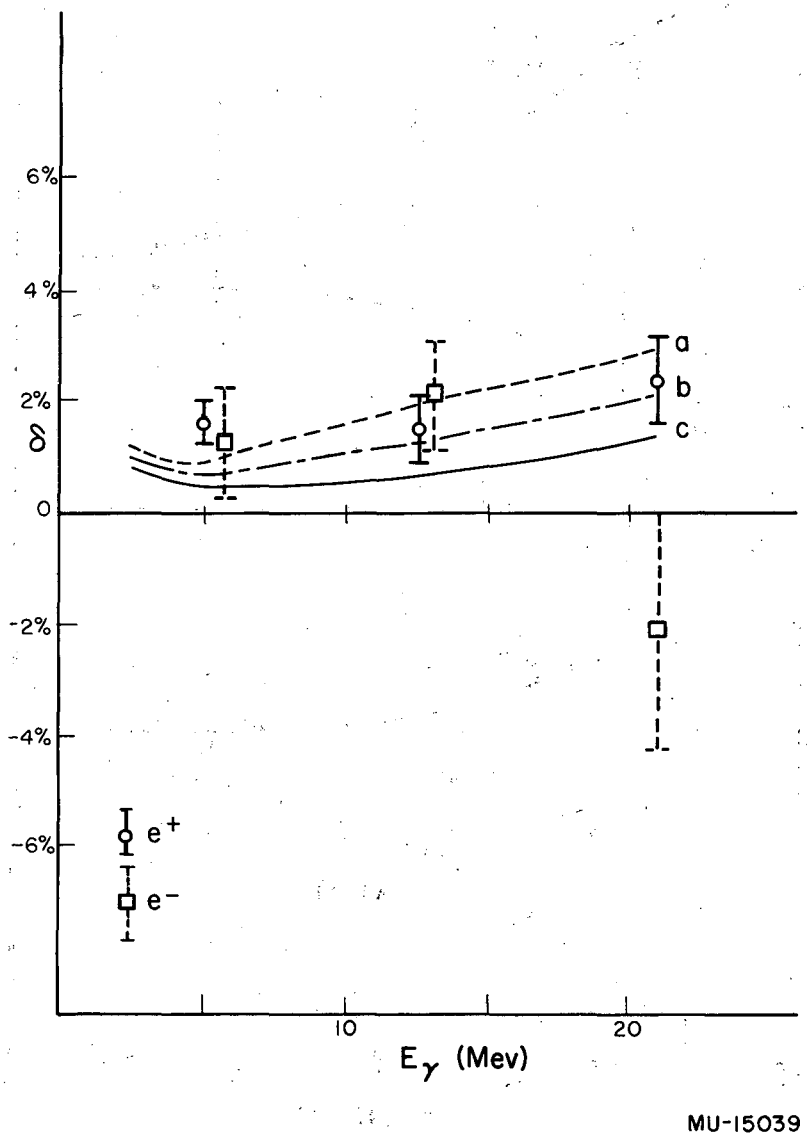

Fig. 10.